

## Research Paper

# Enhanced EGFR inhibition and distinct epitope recognition by EGFR antagonistic mAbs C225 and 425

Vishal Kamat,<sup>1</sup> Joshua M. Donaldson,<sup>2</sup> Csaba Kari,<sup>3</sup> Marlene R.D. Quadros,<sup>4</sup> Peter I. Lelkes,<sup>1</sup> Irwin Chaiken,<sup>5</sup> Simon Cocklin,<sup>5</sup> John C. Williams,<sup>2</sup> Elisabeth Papazoglou<sup>1</sup> and Ulrich Rodeck<sup>3,\*</sup>

<sup>1</sup>School of Biomedical Engineering, Science & Health Systems; Drexel University; Philadelphia, Pennsylvania USA; <sup>2</sup>Department of Biochemistry and Molecular Biology; <sup>3</sup>Department of Dermatology & Cutaneous Biology; <sup>4</sup>Department of Radiation Oncology; Thomas Jefferson University, Philadelphia, Pennsylvania USA; <sup>5</sup>Department of Biochemistry; Drexel University; Philadelphia, Pennsylvania USA

**Abbreviations:** mAbs, monoclonal antibodies; Fab, fragment antigen binding; C225, Erbitux/Cetuximab; 425, Matuzumab/EMD55900; EGFR, epidermal growth factor receptor; sEGFR, soluble extracellular EGFR fragment; AG1478, tyrphostin, EGFR small molecule kinase specific inhibitor

**Key words:** EGFR, antagonist antibodies, epitope mapping, C225, 425, synergy

Monoclonal antibodies (mAbs) that inhibit activation of the epidermal growth factor receptor (EGFR) have shown therapeutic potential in select malignancies including breast cancer. Here, we describe that combined use of two such mAbs, C225 (Cetuximab) and 425 (EMD55900), reduced growth and survival of EGFR overexpressing MDA-MB-468 breast cancer cells more effectively than either antibody alone. Similarly, the C225/425 antibody combination more effectively inhibited AKT and MAPK phosphorylation in MDA-MB-468 cells. Surface plasmon resonance, size exclusion chromatography and analytical ultracentrifugation demonstrated that mAbs C225 and 425 simultaneously bind to distinct antigenic epitopes on domain III of the soluble wild-type EGFR. Furthermore, neither mAb competed with the other for binding to cells expressing either wild-type EGFR or a mutant EGFR (EGFRvIII) associated with neoplasia. Mutagenesis experiments revealed that residues S460/G461 in EGFR domain III are essential components of the 425 epitope and clearly distinguish it from the EGF/TGF $\alpha$  binding site and the C225 interaction interface. Collectively, these results support the conclusion that therapeutic EGFR blockade in cancer patients by combined use of mAbs C225 and 425 could provide advantages over the use of the two antibodies as single agents.

## Introduction

The epidermal growth factor receptor (EGFR; ErbB-1; HER1) is one of four members of the ErbB receptor family and contributes to growth, survival, migration and differentiation of epithelial cells.<sup>1</sup> Deregulated signaling through the EGFR either alone or in cooperation with other members of the ErbB family, notably ErbB2

and ErbB3, is a hallmark of multiple neoplasms predominantly of epithelial origin. The molecular mechanisms leading to deregulated EGFR-dependent signaling include overexpression of the EGFR, establishment of autocrine loops by aberrant overexpression of EGFR ligands and, the expression of mutated, constitutively active EGFRs (reviewed in refs. 2–4).

In recognition of the potential roles of aberrant EGFR activation in tumor progression, multiple antagonists of EGFR activation have been developed with therapeutic intent. These can be broadly divided into two classes: (i) small molecules that target the kinase domain of the EGFR and inhibit its phosphorylation activity and (ii) monoclonal antibodies (mAbs) binding to the extracellular domain of the EGFR (reviewed in ref. 5). Typically, EGFR antagonistic mAbs were selected to disrupt ligand binding to the extracellular domain of the wild-type EGFR. The murine mAb 225 was originally developed by Dr. J. Mendelsohn.<sup>6</sup> A chimeric version of 225 (C225; Cetuximab; Erbitux) containing a human Fc fragment has been FDA-approved for treatment of several epithelial neoplasias including colorectal carcinoma. The murine mAb 425 was developed by us,<sup>7,8</sup> and a humanized version of 425 (EMD72000; Matuzumab) is currently in Phase II clinical trials in various epithelial neoplasms.

Clinical studies with either antibody alone showed promise when they were used as single agents or in the adjuvant setting, raising the issue whether targeting the EGFR with a combination of Cetuximab and Matuzumab may provide added benefit. In support of this notion we demonstrate in the present study that (i) C225 and 425 in combination more effectively inhibit metabolic activity and induce apoptosis of breast cancer cells overexpressing the EGFR, (ii) C225 and 425 bind to separate epitopes on the wild-type EGFR as well as on the mutated, constitutively active EGFRvIII and, (iii) the 425 binding epitope is distinct from the C225 binding site and requires residues S460/G461 present in the human but not the murine EGFR.

## Results and Discussion

**Cooperative inhibition of growth and survival of MDA-MB-468 breast carcinoma cells by mAbs 425 and C225.** In recent years,

\*Correspondence to: Ulrich Rodeck; 233 S. 10<sup>th</sup> Street; BLSB409 Philadelphia, Pennsylvania 19107 USA; Tel.: 215.503.5622; Email: Ulrich.Rodeck@mail.tju.edu

Submitted: 03/20/08; Accepted: 04/14/08

Previously published online as a *Cancer Biology & Therapy* E-publication: <http://www.landesbioscience.com/journals/cbt/article/6097>

combinations of mAbs binding to different epitopes of the same antigen have proven to exert synergistic effects against tumor cells expressing their cognate antigens at the cell surface. For example, two antibodies to ErbB2 (i.e., Trastuzumab and Pertuzumab) inhibit survival of breast cancer cells more effectively than either antibody alone.<sup>14</sup>

Here we investigated whether two antibodies, i.e., 425 and C225, selected independently for the capacity to inhibit ligand binding to the EGFR would similarly affect breast tumor cell growth and survival. In earlier work, detailed characterization of the C225 binding epitope revealed direct competition with EGF/TGF $\alpha$  for binding to domain III of the extracellular portion of the EGFR.<sup>15,16</sup> MAb 425 was similarly selected for interfering with ligand access to the EGFR.<sup>7</sup> However, the binding site for 425 is currently unknown. We compared the effects of either antibody alone with those of the combination of both antibodies on growth and survival of MDA-MB-468 breast carcinoma cells that express high levels of EGFR.<sup>17</sup> To avoid effects due to differences in antibody concentration the total amount of IgG was kept constant for all experimental conditions. As shown in Figure 1A, the combination of the two antibodies was superior to either antibody alone in inhibiting metabolic activity of actively growing, attached MDA-MB-468 cells. The synergistic effect of the antibody combination at 25% growth inhibition is demonstrated by isobologram which depicts equally effective dose pairs (isoboles; Fig. 1B). In this representation, the concentration of one drug required to produce a desired effect is plotted on the horizontal axis while the concentration of another drug producing the same effect is plotted on the vertical axis. A straight line joining these two points represents additive effects expected by the combination of two drugs. Figure 1B shows that, at 25% growth inhibition, the experimental value for the antibody combination lies well below the theoretical additive line consistent with drug synergism. These results demonstrate that the combination of the two antibodies is superior to either antibody alone in inhibiting metabolic activity of actively growing MDA-MB-468 cells.

Next we assayed the capacity of the antibody combination to induce cell death in the anchorage-independent state (Fig. 1C). We demonstrated previously that EGFR inhibition with either 425 (10  $\mu$ g/ml) or with small molecule tyrosine kinase inhibitors accelerates apoptosis of epithelial cells maintained in forced suspension culture which precludes extracellular matrix attachment.<sup>11,18</sup> A simple method to assay cell survival in these conditions consists of reseeding cells on tissue culture-treated plastic after defined periods of suspension culture and the determination of cell reattachment after 12–24 h. This analysis revealed that treatment with either antibody at 10  $\mu$ g/ml during suspension culture reduced the number of cells

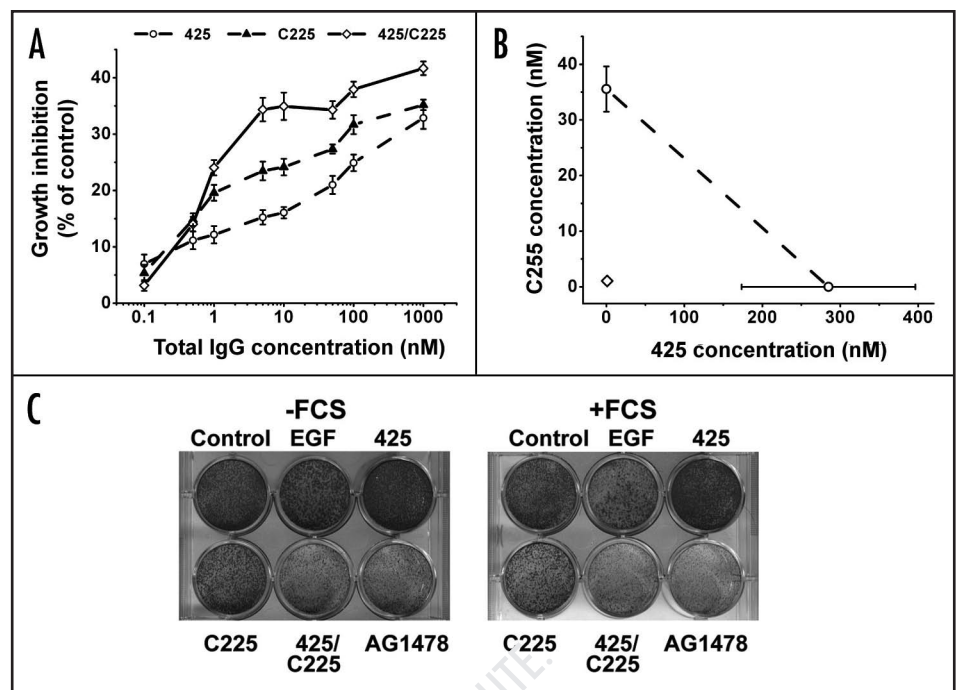


Figure 1. Combinatorial effects of mAbs 425 and C225 on proliferation and anchorage-independent cell survival of MDA-MB-468 breast cancer cells. (A) Dose-dependent effects of either antibody alone at 10  $\mu$ g/ml and the antibody combination at 10  $\mu$ g/ml on metabolic activity as determined by WST-1 assay; the experiment was performed three times and results shown as  $m \pm SEM$ . (B) Isobolographic representation of synergistic antibody effects at 25% growth inhibition. (C) Impaired survival of MDA-MB-468 cells in forced suspension culture in the presence of the 425/C225 combination. In these experiments, the EGFR selective kinase inhibitor, AG1478, was used as a positive control. The capacity of cells to reattach and resume proliferation after two days of forced suspension culture in the presence or absence of 10% FCS was determined. Reattached cells were visualized by crystal violet staining 24 h after re-seeding on cell culture-treated plastic.

capable of matrix reattachment only marginally irrespective of the culture medium used in these experiments (Fig. 1C). In contrast, the combination of both antibodies where each antibody was used at 5  $\mu$ g/ml markedly reduced levels of viable reattached cells similar to cultures treated with the small molecule EGFR inhibitor AG1478. This result indicates that the antibody combination accelerates death of MDA-MB-468 cells in the anchorage-independent state.

**Inhibitory effects of the C225/425 antibody combination on signal transduction events triggered by EGFR activation.** To account for combinatorial inhibitory effects of the antibody combination on EGFR-dependent signal transduction events we determined the effects of the antibodies used either singly or in combination on short-term EGF-induced signal transduction events in serum-starved MDA-MB-468 cells. This analysis revealed more efficient inhibition of AKT and p42/44MAPK phosphorylation in serum-starved cells exposed to EGF and the antibody combination as compared to single antibody treatment (Fig. 2). In fact, in MDA-MB-468 cells, 425 treatment alone did not inhibit AKT and MAPK phosphorylation whereas it very effectively reduced EGF-dependent phosphorylation of the EGFR on Y1068. As in the case of cell growth inhibition experiments the effects on signal transduction events occurred although either antibody was used at half the concentration (5  $\mu$ g/ml) when combined as compared to single antibody treatments (10  $\mu$ g/ml). Overall, the antibody combination

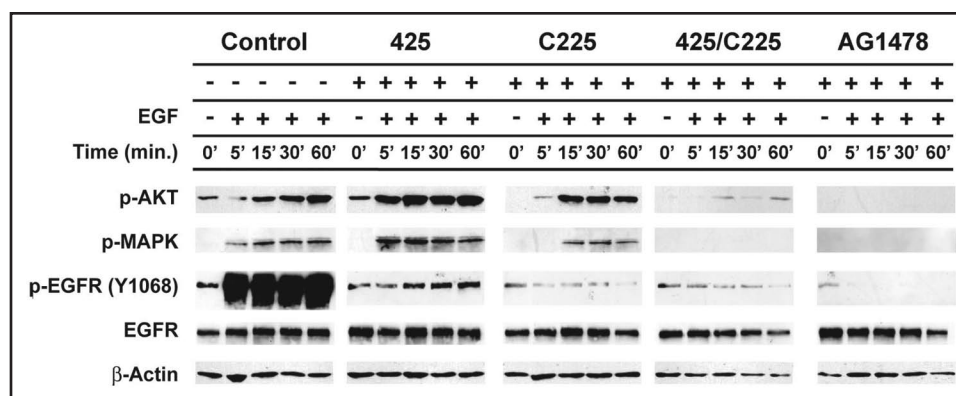


Figure 2. Effects of mAbs 425 and C225 alone and in combination on signal transduction events upon EGF treatment of MDA-MB-468 cells. Phosphorylation of signaling intermediaries (p-AKT473; p-42/44MAPK; p-EGFR Y1068) was determined by immunoblot analysis using phosphospecific antibodies for up to one h after addition of EGF (10 ng/ml) to cells. Comparable loading of wells was assessed using antibodies recognizing the EGFR and  $\beta$ -actin, respectively. Use of the antibody combination amplified inhibitory effects of C225 on AKT and MAPK phosphorylation. Representative results of experiments performed three times are shown.

effects were similar to those achieved by using AG1478 at very high concentration (10  $\mu$ M).

**Simultaneous binding of 425 and C225 to the extracellular domain of the EGFR.** Cooperative growth inhibitory effects by the two antibodies under investigation here could be explained by binding of these antibodies to distinct EGFR populations thus providing more effective ligand binding competition. Alternatively, the two antibodies could simultaneously engage distinct epitopes of the EGFR domain III and inhibit EGFR-dependent signal transduction by independent mechanisms. To distinguish between these two possibilities we performed surface plasmon resonance experiments whereby either antibody was immobilized on a CM5 chip and successive binding of soluble extracellular domain of the EGFR and the second antibody was monitored. To calibrate the system we first characterized binding of sEGFR to either 425 or C225 immobilized on the chip (Fig. 3A and B). In these experiments, lower RUs (~200 RU) of mAbs were conjugated to avoid mass transport limitations. Also, sEGFR was injected at a high flow rate of 50  $\mu$ l/min in order to overcome potential receptor rebinding effects. The resultant sensorgrams were then analyzed and the equilibrium rate constants were calculated. The real time sensorgrams were pseudocolored for different concentrations of injected sEGFR while the calculated kinetic fit of the interaction is represented in black. Analysis of the binding data revealed that C225 binds to sEGFR with a higher affinity ( $2.7 \pm 0.4$  nM) compared to 425 ( $32.3 \pm 6.75$  nM) due to a comparatively higher dissociation rate of 425. The binding affinity of C225 as determined by these analyses was very similar to that previously described.<sup>16</sup>

The next set of experiments focused on the question whether sEGFR bound to C225 immobilized on the chip was capable of capturing 425. To this end, sEGFR (5 nM) was injected over a low-density C225 chip (280 RU) followed by different concentrations of 425 (0–512 nM) until binding equilibrium was reached. The sensorgrams reveal binding of concentration-dependent binding of 425 to sEGFR captured by C225 (Fig. 3C), consistent with non-competitive binding of the two antibodies to sEGFR.

To obtain independent confirmation for simultaneous binding of both antibodies to EGFR we performed sedimentation equilibrium analysis by analytical ultracentrifugation using an admixture

of C225, 425 and the extracellular portion of the EGFR consisting of domains I to IV (sEGFR). This analysis indicated a single species with an apparent weight of 167 kD, consistent with the existence of a 1:1:1 tripartite molecular complex (Fig. 4). Note that total concentration was at 4.5  $\mu$ M or >100-fold and >1000-fold the dissociation constant of 425 or C225 and EGFR, respectively. Together, these results strongly suggest that the binding epitopes of C225 and 425 are distinct albeit both are confined to domain III of the extracellular portion of the human EGFR.<sup>19</sup>

Next we addressed the question whether both antibodies could also simultaneously engage the EGFR expressed on cell surfaces. To this end, we used NIH3T3 cells stably transfected with either full-length wild-type human EGFR (CO12 cells) or an mutated EGFR characterized by intragenic deletion of most of domain II of the EGFR and prominently expressed in neoplasia (HC2 cells).<sup>9</sup> As both antibodies bind exclusively to domain III of the EGFR<sup>19</sup> we expected that they would not only bind to wild-type but also the tumor-specific EGFRvIII. To avoid confounding effects of endogenous EGFR expression we used transfected mouse 3T3 cells in these experiments rather than human cells. Since both antibodies under investigation do not recognize the murine EGFR<sup>7,20</sup> no binding other than to the transfected human EGFR is measured. To assess direct binding competition between the two antibodies we determined by FACS analysis the capacity of 425 to replace C225 from the cell surface of CO12 and HC2 cells. This analysis revealed the expected result in that either antibody competed with itself for cell surface binding but not with the other (Fig. 5). In addition and as expected both antibodies recognized both, human wild-type EGFR and EGFRvIII. Collectively, these results indicate simultaneous binding of the two antibodies under investigation to distinct epitopes on domain III of the extracellular portion of recombinant human EGFR and cell-associated EGFR.

**MAb 425 recognizes an EGFR epitope distinct from the ligand binding domain.** The results described above are consistent with independent and simultaneous engagement of the EGFR by both antibodies under investigation. C225 is known to directly compete with ligand binding to domain III of the EGFR.<sup>16</sup> In contrast, whereas 425 is known to bind to domain III, its epitope has yet to



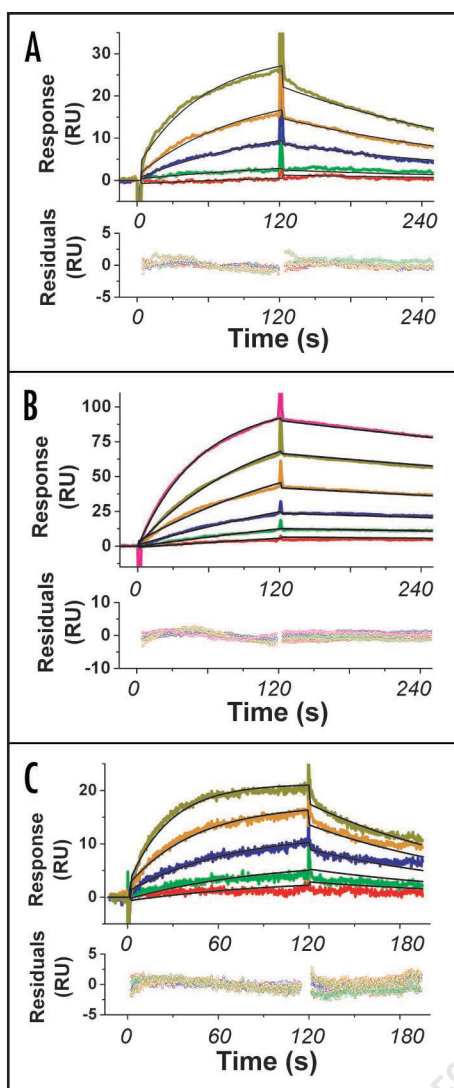


Figure 3. Simultaneous binding of mAbs C225 and 425 to the extracellular portion of the EGFR (sEGFR). (A) Surface plasmon resonance analysis of sEGFR captured by 425 tethered on CM5 chips. The real time sensorgram is colored for different sEGFR concentrations and the calculated fit using the model of 1:1 Langmuir binding with mass transport limitation is shown in black. The residuals of the fit are provided under the sensorgram. For calculation of binding affinities please refer to Table 1. (B) Surface plasmon resonance analysis of sEGFR captured by C225 bound to CM5 chips. (C) Binding of 425 to sEGFR captured by C225. Approximately 30 RUs of sEGFR were captured on a C225 immobilized CM5 chip and used as ligand to study the binding kinetics of mAb 425. Increasing concentrations of 425 were injected at 20  $\mu$ l/min for two minutes association time and two minutes dissociation time. All Biacore experiments shown were conducted at least three times with similar results.

be defined. We inferred that the 425 binding site must encompass residues that are different in the human and murine EGFR sequences as 425 recognizes a conformationally defined epitope of the human but not the murine EGFR.<sup>7</sup> Thus, residues that differ between the murine and human sequences and are present on the surface of the sEGFR domain III are likely candidates for the epitope defined by 425 binding. In addition, our data shows C225 and 425 bind simultaneously to the surface of EGFR domain III indicating that the 425 epitope must lie outside of the surface masked by C225.

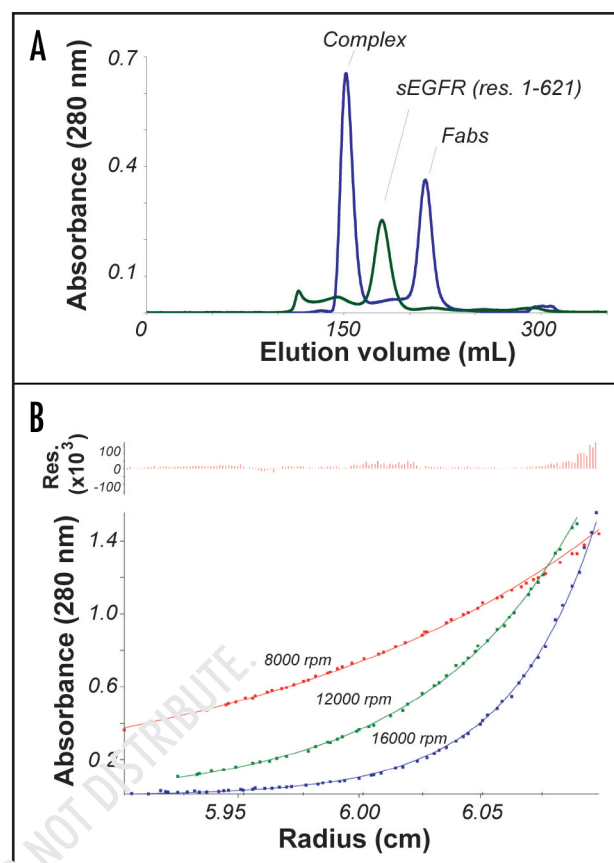


Figure 4. Sedimentation equilibrium analysis of complexes formed by C225 and 425 Fabs and the extracellular portion of EGFR (sEGFR). (A) The complex was formed by saturating sEGFR with Fab fragments of C225 and 425 and isolated by size exclusion chromatography. (B) Radial scans at 280 nm were collected at 8000 (red), 12000 (green) and 16000 (blue) RPM at 20°C. The data fit well to a single molecular species and afforded a calculated molecular weight of 167,100  $\pm$  1000 Da, consistent with a tripartite complex.

Mapping of the human EGFR using these constraints produced a handful of potential EGFR/425 interaction sites (Fig. 6). Many of these sites are located near glycosylation sites and were considered unlikely targets for 425 binding because we previously showed that 425 recognizes a protein epitope on the deglycosylated EGFR.<sup>7</sup> After exclusion of residues occluded by either C225 or by putative carbohydrate side chains, two adjacent amino acids emerged as likely candidates for 425 docking (Ser460 and Gly461 highlighted in Fig. 6). To investigate the role of these residues in 425 binding, we changed these two residues in human EGFR domain III to the corresponding murine sequence, (i.e., Pro460 and Asn461), expressed and purified this domain, and used size exclusion chromatography to test whether 425 could bind sEGFR domain III encoding S460P and G461N mutations (Fig. 7). The individual Fabs and sEGFR domain III proteins eluted at 15.6 mL. Co-incubation of sEGFR domain III<sup>S460P/G461N</sup> with Fab425 resulted in a slightly earlier elution, 15.2 mL, indicating weak association. Note that the concentration of the mixture added to the column is 4  $\mu$ M or 125-fold greater than the  $K_D$  of the native EGFR/425 interaction. Thus, some weak association is expected. As a point of reference, mutations that define the C225 epitope on EGFR-domain III reduced the affinity from 2.3

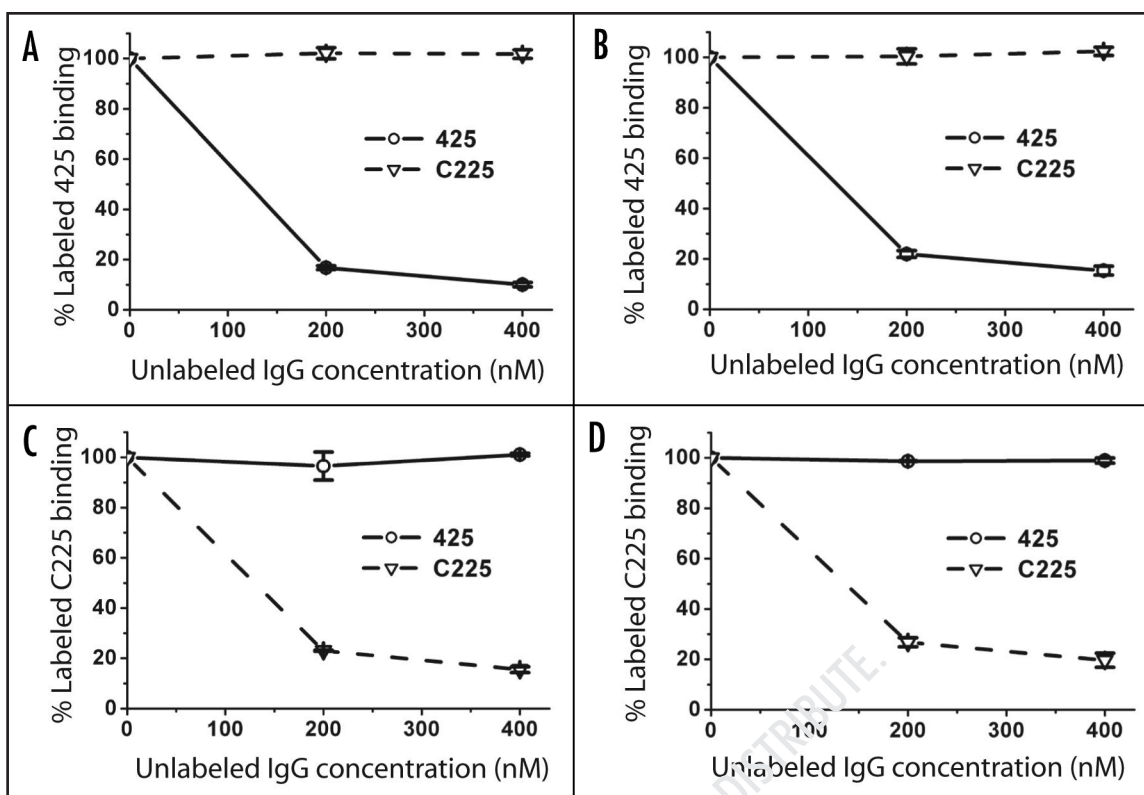


Figure 5. Independent binding of mAbs C225 and 425 to the human EGFR expressed on cell surfaces. Binding of Alexa Fluor 488-labeled C225 and 425 was assessed by FACS in the presence of unlabeled C225 or 425 as indicated in the panels. This analysis was performed using NIH3T3 cells engineered to express wild-type human EGFR (HC2; A and B) or the tumor-specific EGFRvIII (CO12; C and D) as indicated. In both cases, either antibody competed with itself but not with the other antibody. A representative example of three experiments is shown.

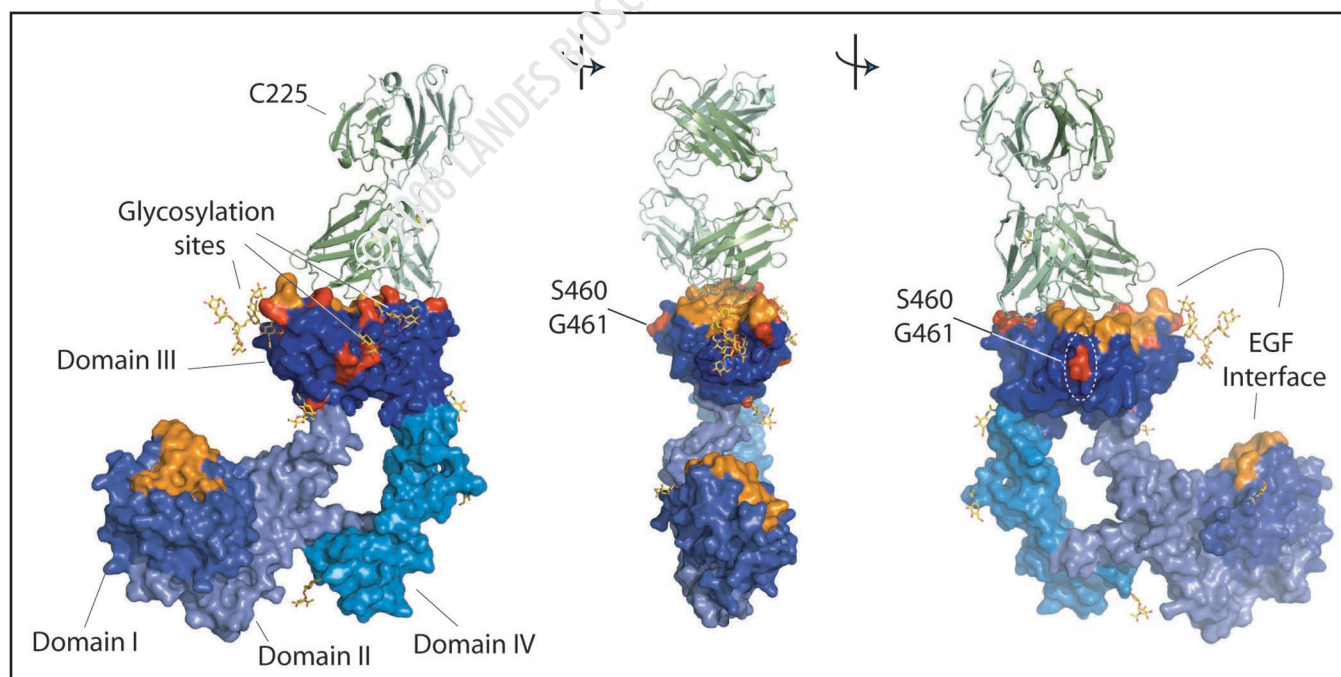


Figure 6. Modeling of the 425 binding site on the EGFR. Surface representation of the extracellular portion of EGFR bound to C225 (ribbon representation) based on the structure 1YY9.<sup>16</sup> Sequence differences between human and murine EGFR domain III are highlighted in red. Glycosylation of asparagine residues found in the structure of 1YY9 are shown as sticks (carbons yellow and oxygen red). The EGF-EGFR interface based on the crystal structure 1IVO<sup>21</sup> and limited to 5 Å cutoff is shown in orange. Note that S460 and G461 represent the only surface residues of interest on domain III that are either not occluded by C225 or likely to be affected by N-linked glycosylation. The figure was made in PyMol.<sup>22</sup>

nM to 340 nM<sup>16</sup> and complex of this mutant and C225 would also show residual binding at concentrations 125 fold greater than the original  $K_D$  (e.g., ~290 nM). However, human sEGFR domain III at the same concentration formed a *saturated* complex that eluted at 13.9 mL. To demonstrate that the point mutations did not affect the tertiary structure of the sEGFR domain III, the S460P and G461N mutant was also mixed with C225 Fab and subjected to analysis by size exclusion chromatography. Its elution point at 14.0 mL is similar to the wild-type sEGFR domain III complexed with C225. Finally, when wild-type sEGFR domain III and both Fabs were mixed and applied to the column, a distinct peak eluting at 13.1 mL emerged, consistent with a tripartite complex. Taken together, these data indicate that Ser460 and Gly461 significantly contribute to the overall affinity of the EGFR-425 interaction.

These results raise the question of how 425 interferes with ligand binding to the EGFR as originally reported by us.<sup>7</sup> As it does not compete with C225 for binding and recognizes surface residues distinct from the ligand binding site, a different mechanism of action may account for its biological effects. Specifically, it is possible that interaction of 425 with the EGFR interferes with high affinity ligand binding by blocking a conformational change to bring domains I and III of the extracellular domain of the EGFR in close proximity.

**Conclusions.** The most salient findings of this work can be summarized as follows: (i) two mAbs to the human EGFR (425 and C225) that are of clinical interest cooperatively inhibit EGFR activation; (ii) the two antibodies in question simultaneously bind to domain III of the extracellular portion of the EGFR; (iii) the 425 epitope on the human EGFR contains amino acid residues G460/S461 and is distinct from both, ligand binding site and C225 binding site. Taken together, the results of this study suggest that the combination of humanized 425 (Matuzumab) and Cetuximab may provide a more effective means to target tumor-associated EGFR in patients.

## Materials and Methods

**Cells and reagents.** Human epithelial breast cancer cells MDA-MB-468 (ATCC HTB-132) were purchased from American Type Culture Collection (ATCC), Rockville, MD, USA. NIH3T3 cells transfected with either full-length human EGFR (CO12) or mutated EGFR variant III (EGFRvIII; HC2) were a generous gift from Dr. Albert Wong.<sup>9</sup> Mab 425 was isolated from murine ascites by affinity purification using Protein A Sepharose columns followed by Ion Exchange columns (GE Health Sciences Q Sepharose 4, fast flow). Purified C225/Cetuximab was purchased from Bristol Myers Squibb, Princeton, NJ. The EGFR selective tyrosine kinase inhibitor, tyrphostin AG1478, was purchased from Calbiochem. For surface plasmon resonance experiments, the extracellular soluble domain of the human EGFR (sEGFR) was purchased from R&D Systems, Inc., WST-1 cell proliferation kit was purchased from Takara Bio Inc.

HC2, CO12, and MDA-MB-468 cells were cultured in DMEM supplemented with 1 g/l glucose, 2 mM L-glutamine, 10% FBS, 1% penicillin/streptomycin under standard conditions.

**Expression of recombinant EGFR fragments.** Soluble EGFR (sEGFR) constructs, extracellular domain (residues 1–621) and domain III, (residues 310–512) were generated, produced and purified closely following published methods.<sup>10</sup> Two point mutations, S460P/G461N, were introduced into sEGFR domain III by site directed mutagenesis using the QuikChange method (Stratagene).

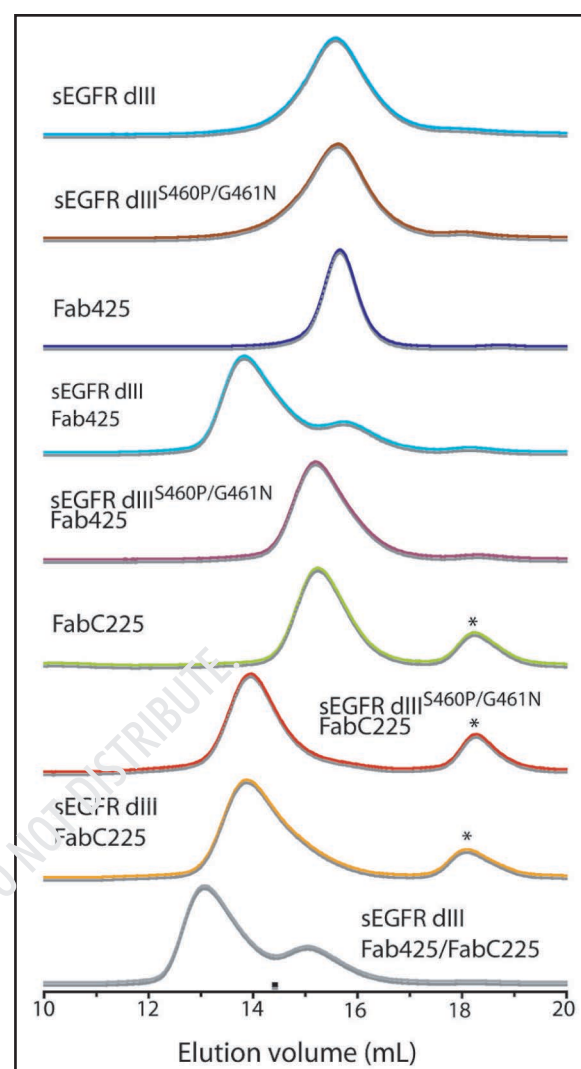


Figure 7. Mab 425 binds the EGFR at an epitope distinct from C225 as determined by size exclusion chromatography. MAb 425 and C225 bind to domain III individually (cyan and orange traces) and as a combination (grey trace). Note that the complex of 425 with the EGFRdIII<sup>S460P/G461N</sup> elutes slightly earlier than the individual components (purple trace), but significantly later than the non-mutated domain III (cyan). The complex of C225 with the mutated EGFRdIII (red) eluted at the same volume as the non-mutated domain III (orange) indicating that the point mutations do not interfere with the overall tertiary structure. Asterisks denote an impurity not present in the C225 preparation. The concentration of each sample added to the column was 4  $\mu$ M (based on absorbance at 280 nm).

**Papain digestion of 425 and C225.** Fab fragments of 425 and C225/Cetuximab were prepared by papain digestion and Protein A reverse purification (Pierce). Each protein was further purified using a HiLoad 16/60 Superdex 75 column.

**Flow cytometry.** Flow cytometric analyses were carried out using mAbs 425 and C225 conjugated to Alexa Fluor 488 through primary amines following the manufacturer's protocol (Molecular Probes). Between 4–6 Alexa 488 molecules were bound per antibody as estimated by measuring the optical density at 280 nm and 494 nm. For FACS analysis, cells were detached using a non-enzymatic cell dissociation solution (Cellgro), collected and resuspended in



wash buffer (1X PBS containing 1% BSA). Approximately 500,000 cells were incubated at 4°C in 50 µl of labeled and unlabeled antibodies as indicated. After 30 min of incubation, cells were washed thrice with wash buffer and fixed using 1% freshly prepared paraformaldehyde. Samples were analyzed on a FACS Canto (BD Biosciences).

**WST-1 assay.** Effects of C225 and 425 on metabolism of MDA-MB-468 were measured by assaying cleavage of the tetrazolium salt WST-1 to fluorescent formazan by cellular mitochondrial dehydrogenases as quantified by measuring the absorbance of the dye solution at 450 nm. In 48-well plates, approximately 3000 cells/well suspended in 200 µl of DMEM containing 10% FCS were allowed to attach for 24 h. After 24 h, 100 µl of antibody solutions diluted in DMEM were added to each well to achieve the desired concentrations. After 72 h 30 µl of WST-1 was added for another three hours. For analysis, 60 µl of culture medium was added to 200 µl of 1xPBS buffer and the absorbance was measured at 450 nm using a Victor2 1420 Multilabel counter (Perkin Elmer). The absorbance at 550 nm was used for background correction. The percent inhibition was calculated as  $100 \times (\text{Abs}_{\text{Control}} - \text{Abs}_{\text{mAb}}) / \text{Abs}_{\text{Control}}$ .

**Anchorage-independent cell growth and survival.** Cell survival in the anchorage-independent state was determined as previously described<sup>11</sup> with minor modifications. Cell suspensions were prepared in DMEM containing 0.2% BSA in the presence and absence of 10% FCS, mAbs 425, C225 or their combination (10 µg/ml final antibody concentration), AG1478 (10 µM) and/or EGF (10 ng/ml). After 48 and 72 h, 500 µl of cell suspension was transferred to another 6-well plate with the respective culture medium and allowed to attach and grow for 24 h. Attached cells were fixed in 75% ethanol and stained with crystal violet.

**Immunoblot analyses.** Cells were incubated in complete growth medium in 100 mm petri dishes (1 x 10<sup>6</sup> cells per dish) for 24 h. After overnight incubation in serum-free DMEM containing 0.2% BSA, antibodies (10 µg/ml final IgG concentration) or AG1478 (10 µM) were added. After one hour, EGF (10 ng/ml final concentration) was added to culture media and cells lysed using Rasmussen buffer. Differences in the phosphorylation of MAPK, AKT and EGFR were determined by immunoblot analysis. Antibody binding was detected using an enhanced chemiluminescence system (Pierce).

**Biacore surface plasmon resonance analysis.** Molecular interactions were determined using a Biacore® 3000 optical biosensor (Biacore Inc.). Immobilization of EGFR specific mAbs to CM5 sensor chips were performed following the standard amine coupling procedure. Unless specified otherwise anti-HIV-1 gp120 antibody 17b immobilized on CM5 chips was used as a reference flow cell.<sup>12</sup> Ligand densities and flow rates were optimized to minimize mass transport and rebinding effects.

Analysis of direct binding of sEGFR in a concentration dependent manner to 425 or C225 was achieved by passage over mAb surfaces with a ligand density of 200 RUs and a flow rate of 50 µl/min for two minutes association and 6 min dissociation at 25°C. Regeneration of the surfaces between injections was achieved by injecting three, six sec pulses of 10 mM glycine, pH 2.0 at the flow rate of 100 µl/min.

To study simultaneous binding of 425 and C225, a capture SPR format was employed. Briefly, sEGFR (5 nM) was injected over a low density C225 surface (280 RUs) at 20 µl/min. The captured sEGFR was then used as ligand to perform saturation analysis by injecting

increasing concentrations of 425 (0–512 nM) for three minutes at a flow rate of 50 µl/min until binding equilibrium ( $R_{eq}$ ) was achieved. Data were analysed using BIAevaluation® 4.0 software (Biacore Inc., NJ). The responses of a buffer injection and responses from a reference flow cell were subtracted to account for nonspecific binding and instrument noise. Experimental data were fitted to a simple 1:1 binding model with a parameter included for mass transport.

**Sedimentation equilibrium analysis.** A complex of full-length sEGFR, Fab425 and FabC225 was incubated for 30 min, applied to a HiLoad 16/60 Superdex 200 prep grade column and loaded into a loaded into a 6-well, analytical centrifugation cell at  $A_{280\text{ nm}} = 1.0$ . The samples were centrifuged using an An-50 Ti rotor at 20°C in a Beckman ProteomeLab XL-I ultracentrifuge. Absorbance scans at 280 nm were performed after 12 and 14 hours at 8000, 12000 and 16000 RPM. Equilibrium was assessed by comparison of scans at 12 and 14 hours. Analysis was performed using FastFitter<sup>13</sup> as implemented in Igor Pro (Wavemetrics, Lake Oswego, OR). The solvent density ( $\rho$ ) was set at 1.0042 g/ml and the specific volume ( $V_{BAR}$ ) was assumed to be 0.76 ml/g.

**Size exclusion chromatography.** Complexes comprised of different combinations of sEGFR domain III, the mutated (S460P/G461N) sEGFR domain III, Fab 425 and Fab C225 were prepared at 4 µM and incubated for 20 min. Size exclusion chromatography was performed at 4°C using a Superdex 200 HR10/30 column (GE Health Sciences) and monitored at 280 nm.

#### Acknowledgements

We thank Dr. James Lear at the University of Pennsylvania for helpful discussion concerning the sedimentation equilibrium experiments. We also thank present and former members of the Rodeck, Williams and Papazoglou laboratories for general support and advice. This work was supported, in part, by grants from the NIH to UR (CA81008) and JCW (RR022316). J.M.D. acknowledges support from the Foerderer Scholar Fellowship Award, the Dubbs Scholar Fellowship Award and the Measey MD/PhD Student Fellowship. Additional support was provided by a seed grant from RTOG and a grant from the State of Pennsylvania to UR and from the Nanotechnology Institute of Southeastern Pennsylvania (NTI) to E.P.

#### References

- Yarden Y, Sliwkowski MX. Untangling the ERBB signalling network. *Nature Reviews Molecular Cell Biology* 2001; 2:127-37.
- Mendelsohn J, Baselga J. The EGF receptor family as targets for cancer therapy. *Oncogene* 2000; 19:6550-65.
- Kim ES, Khuri FR, Herbst RS. Epidermal growth factor receptor biology (IMC-C225). *Curr Opin Oncol* 2001; 13:506-13.
- Nagane M, Lin H, Cavenee WK, Huang HJ. Aberrant receptor signaling in human malignant gliomas: mechanisms and therapeutic implications. *Cancer Lett* 2001; 162:17-21.
- Baselga J, Arteaga CL. Critical update and emerging trends in epidermal growth factor receptor targeting in cancer. *J Clin Oncol* 2005; 23:2445-59.
- Masui H, Kawamoto T, Sato JD, Wolf B, Sato G, Mendelsohn J. Growth inhibition of human tumor cells in athymic mice by anti-epidermal growth factor receptor monoclonal antibodies. *Cancer Res* 1984; 44:1002-7.
- Murthy U, Basu A, Rodeck U, Herlyn M, Ross AH, Das M. Binding of an antagonistic monoclonal antibody to an intact and fragmented EGF-receptor polypeptide. *Arch Biochem Biophys* 1987; 252:549-60.
- Rodeck U, Herlyn M, Herlyn D, Molthoff C, Atkinson B, Varello M, Stepelwski Z, Koprowski H. Tumor growth modulation by a monoclonal antibody to the epidermal growth factor receptor: immunologically mediated and effector cell-independent effects. *Cancer Res* 1987; 47:3692-6.
- Moscatoello DK, Montgomery RB, Sundareshan P, McDanel H, Wong MY, Wong AJ. Transformatonal and altered signal transduction by a naturally occurring mutant EGF receptor. *Oncogene* 1996; 13:85-96.

10. Ferguson KM. Active and inactive conformations of the epidermal growth factor receptor. *Biochem Soc Trans* 2004; 32:742-5.
11. Jost M, Huggett TM, Kari C, Rodeck U. Matrix-independent survival of human keratinocytes through an EGF receptor/MAPK-Kinase-dependent pathway. *Molecular Biology of the Cell* 2001; 12:1519-27.
12. Thali M, Moore JP, Furman C, Charles M, Ho DD, Robinson J, Sodroski J. Characterization of conserved human immunodeficiency virus type 1 gp120 neutralization epitopes exposed upon gp120-CD4 binding. *J Virol* 1993; 67:3978-88.
13. Arkin M, Lear JD. A new data analysis method to determine binding constants of small molecules to proteins using equilibrium analytical ultracentrifugation with absorption optics. *Anal Biochem* 2001; 299:98-107.
14. Nahta R, Hung MC, Esteva FJ. The HER-2-Targeting Antibodies Trastuzumab and Pertuzumab Synergistically Inhibit the Survival of Breast Cancer Cells. *Cancer Res* 2004; 64:2343-6.
15. Gill GN, Kawamoto T, Cochet C, Le A, Sato JD, Masui H, McLeod C, Mendelsohn J. Monoclonal anti-epidermal growth factor receptor antibodies which are inhibitors of epidermal growth factor binding and antagonists of epidermal growth factor binding and antagonists of epidermal growth factor-stimulated tyrosine protein kinase activity. *Journal of Biological Chemistry* 1984; 259:7755-60.
16. Li S, Schmitz KR, Jeffrey PD, Wiltzius JJ, Kussie P, Ferguson KM. Structural basis for inhibition of the epidermal growth factor receptor by cetuximab. *Cancer Cell* 2005; 7:301-11.
17. Biscardi JS, Belsches AP, Parsons SJ. Characterization of human epidermal growth factor receptor and c-Src interactions in human breast tumor cells. *Mol Carcinog* 1998; 21:261-72.
18. Jost M, Huggett TM, Kari C, Boise LH, Rodeck U. Epidermal growth factor receptor-dependent control of keratinocyte survival and Bcl-x<sub>L</sub> expression through a MEK-dependent pathway. *Journal of Biological Chemistry* 2001; 276:6320-6.
19. Lax I, Fischer R, Ng C, Segre J, Ullrich A, Givol D, Schlessinger J. Noncontiguous regions in the extracellular domain of EGF receptor define ligand-binding specificity. *Cell Regul* 1991; 2:337-45.
20. Wen X, Wu QP, Ke S, Ellis L, Charnsangavej C, Delpassand AS, Wallace S, Li C. Conjugation with (111)In-DTPA-poly(ethylene glycol) improves imaging of anti-EGF receptor antibody C225. *J Nucl Med* 2001; 42:1530-7.
21. Ogiso H, Ishitani R, Nureki O, Fukai S, Yamanaka M, Kim JH, Saito K, Sakamoto A, Inoue M, Shirouzu M, Yokoyama S. Crystal structure of the complex of human epidermal growth factor and receptor extracellular domains. *Cell* 2002; 110:775-87.
22. DeLano WL. Unraveling hot spots in binding interfaces: progress and challenges. *Curr Opin Struct Biol* 2002; 12:14-20.

©2008 LANDES BIOSCIENCE. DO NOT DISTRIBUTE.